JB
Journals.ASM.org

Multiple Envelope Stress Response Pathways Are Activated in an *Escherichia coli* Strain with Mutations in Two Members of the DedA Membrane Protein Family

Rakesh Sikdar, Angelica R. Simmons, William T. Doerrler

Department of Biological Sciences, Louisiana State University, Baton Rouge, Louisiana, USA

We have reported that simultaneous deletion of two *Escherichia coli* genes, *yqjA* and *yghB*, encoding related and conserved inner membrane proteins belonging to the DedA protein family results in a number of intriguing phenotypes, including temperature sensitivity at 42°C, altered membrane lipid composition, and cell division defects. We sought to characterize these and other phenotypes in an effort to establish a function for this protein family in *E. coli*. Here, using reporter assays, we show that the major envelope stress response pathways Cpx, Psp, Bae, and Rcs are activated in strain BC202 (W3110; Δ*yqjA* Δ*yghB*) at the permissive growth temperature of 30°C. We previously demonstrated that 10 mM Mg^{2+}, 400 mM NaCl, and overexpression of *tatABC* are capable of restoring normal growth to BC202 at elevated growth temperatures. Deletion of the *cpxR* gene from BC202 results in the loss of the ability of these supplements to restore growth at 42°C. Additionally, we report that the membrane potential of BC202 is significantly reduced and that cell division and growth can be restored either by expression of the multidrug transporter MdfA from a multicopy plasmid or by growth at pH 6.0. Together, these results suggest that the DedA family proteins YqjA and YghB are required for general envelope maintenance and homeostasis of the proton motive force under a variety of growth conditions.

Integral membrane proteins make up 20 to 25% of all predicted open reading frames (1). Some are restricted to one or a few closely related species, while others are conserved across diverse phylogenies. The DedA membrane protein family falls into the latter class and is represented in nearly all sequenced bacterial genomes, as well as the genomes of many archaea and eukaryotes (see the accompanying paper by Doerrler et al. [81]). At present, there are more than 3,000 members of the DedA family found in the NCBI genome database (2). The precise functions of the DedA family remain enigmatic, but some clues have come from studies involving bacterial genetics.

The *Escherichia coli* genome carries eight genes (*dedA*, *yqjA*, *yghB*, *yohD*, *yabI*, *ydjX*, *ydjZ*, *yqaA*) which encode proteins belonging to the DedA family, with levels of amino acid identity ranging from 25% to 60%. While all are individually nonessential genes (3), we reported that simultaneous deletion of *yqjA* and *yghB* (strain BC202), encoding integral inner membrane proteins with ~60% amino acid identity, results in cell division defects at all growth temperatures and loss of growth at 42°C (4). We demonstrated that the altered cell division is due to inefficient secretion of periplasmic amidases by the twin arginine transport (Tat) pathway (5) in spite of the fact that neither YqjA nor YghB is believed to play a direct role in the Tat pathway itself (6). We have recently demonstrated the essentiality of the DedA protein family in *E. coli*. While *E. coli* can survive with only one DedA family gene, the loss of all 8 members of the family results in loss of viability and cell lysis (7).

As mentioned, the DedA family is conserved across most bacterial phyla, and *E. coli* and many bacterial species have multiple DedA homologues. However, the genome of the Lyme disease pathogen *Borrelia burgdorferi* encodes only a single DedA homolog (annotated *bb0250*) (8). We showed that cloned *bb0250* rescues the temperature sensitivity and cell division defects of BC202 despite encoding a protein with only 19% amino acid identity to YqjA (9). In addition, *bb0250* is an essential gene in *Borrelia* and depletion of the protein product expressed from an inducible promoter results in cell death preceded by cell division defects (9). These results from *B. burgdorferi* and *E. coli* demonstrate that the functions of DedA family proteins are critical for cell survival and are conserved across distant bacterial species. Intriguingly, these phenotypes described above for the *Borrelia* DedA mutant are independent of any role these proteins may play in the Tat protein export pathway, since the *B. burgdorferi* genome does not encode homologs of the *E. coli* Tat components TatABCDE or any proteins with predicted Tat-dependent signal peptides (10). Other phenotypes of BC202 suggest that YqjA and YghB play more general roles in *E. coli* instead of a specific role in the Tat pathway. ΔTat mutants, like BC202, are viable and display cell division defects due to loss of periplasmic amidases but, unlike BC202, can grow at all temperatures (11–13). Additionally, BC202 displays an altered membrane phospholipid composition with elevated levels of acidic phospholipids phosphatidylglycerol (PG) and cardiolipin (CL) and reduced amounts of zwitterionic phosphatidylethanolamine (PE) (4).

In an effort to explain the temperature sensitivity of BC202 and explore the function of the DedA protein family in *E. coli*, we measured the activation of several well-characterized stress response pathways in BC202. *E. coli* responds to extracytoplasmic

Received 2 May 2012 **Accepted** 28 September 2012

Published ahead of print 5 October 2012

Address correspondence to William T. Doerrler, wdoerr@lsu.edu.

Supplemental material for this article may be found at http://dx.doi.org/10.1128/JB.00762-12.

doi:10.1128/JB.00762-12

stress by activating one or more of several well-known stress response pathways such as the σ^E, Cpx, Psp, Bae, and Rcs stress response pathways, which help the cells detect and combat alterations in their cell envelope when challenged with a plethora of conditions that compromise envelope integrity (14). The Cpx and σ^E pathways are activated in response to disruptions in the folding of envelope proteins and loss of outer membrane integrity and have partially overlapping regulons (14–17). The σ^E stress response is mediated by transcriptional regulation of target genes by the alternative sigma factor σ^E (18), while the CpxAR two-component system is responsible for the Cpx stress response, with CpxA being the histidine kinase sensor and CpxR being the response regulator (17). The broad and varied content of the Cpx regulon (19) and recent discoveries which revealed that the Cpx pathway is also activated in response to a variety of diverse signals such as adhesion (20), onset of stationary phase (21), and growth in the presence of excess carbon source such as pyruvate or glucose (22) have broadened the known range and scope of this stress response pathway.

The Psp (phage shock protein) response is activated by perturbations in the integrity of the inner membrane by stress conditions (e.g., extreme heat shock, exposure to ethanol, ionophores, and pIV secretin stress), which results in dissipation of the proton motive force (pmf) and changes the physiological redox state of the cell (23–25). The primary function of the Psp stress response pathway is to employ countermeasures when bacteria are challenged with conditions which can potentially dissipate the pmf by compromising envelope integrity (26). The Psp stress response system is comprised of the PspABCDE, PspF, and PspG proteins (26). The response regulator PspF enhances σ^{54}-dependent transcription of the *psp* operon. PspA acts as the negative regulator by binding to PspF in the absence of stress signals. Inner membrane sensors PspB and PspC and the periplasmic sensor protein PspE (27) are proposed to sense the stress signals and transduce them to the PspF-PspA inhibitory complex, resulting in release of PspF (26). PspA also binds to the phospholipids of the inner leaflet of the inner membrane and prevents proton leakage (14, 28).

The Rcs (regulator of colanic acid synthesis) pathway is a complex phosphorelay which participates in extracytoplasmic stress response. It has been shown to be activated by stresses which affect envelope composition (29–32) or stresses which compromise murein integrity (33). In addition, interaction with solid surfaces (30), acid stress, hyperosmotic shock (34) and changes in the phosphorylation of undecaprenyl carrier lipid (35) can also trigger Rcs activation. The main components of this stress response system are the outer membrane (OM) lipoprotein RcsF (stress sensor/transducer) (36), RcsC (hybrid sensor with a histidine kinase transmitter and an aspartate receiver domain), RcsD (signal transducer from RcsC to RcsB), and RcsB and RcsA (transcriptional response regulators) (14, 30). The colanic acid biosynthesis genes (*cps*) are regulated by RcsA in an RcsB-dependent manner which results in overproduction of capsular polysaccharide, resulting in the familiar mucoid phenotype of *E. coli* colonies in response to Rcs activation (30).

The Bae (bacterial adaptive response) pathway is mediated by the BaeSR two-component system, comprising the BaeS histidine kinase sensor and the BaeR response regulator. Bae stress response is induced by exposure to toxic compounds such as indole and ethanol and regulates the expression of genes encoding multidrug transporters such as the *mdtABCD* operon, *acrD*, and *emrK* in addition to OM porin TolC and periplasmic chaperone Spy along with a few other conserved proteins (14, 37, 38).

The bacterial envelope stress response pathways sense a variety of stresses which impair envelope integrity. They respond to these stresses by regulating complementary physiological functions necessary for mounting a complete adaptive response. They also modulate necessary physiological functions such as bacterial adhesion, biofilm formation, motility, conjugation, stationary-phase adaptation, virulence, etc. (14). We report in this study that envelope stress response pathways Cpx, Psp, Rcs, and Bae are strongly induced in BC202 under permissive growth conditions whereas σ^E is repressed (likely due to Cpx activation). This type of nonspecific induction of multiple envelope stress responses is reminiscent of a general loss of envelope integrity when challenged with certain growth conditions such as growth in 5% ethanol (14).

In addition, we demonstrate that the membrane potential is significantly lowered in BC202 under normal growth conditions. We propose that the phenotypes of BC202 result from an inefficient pmf homeostasis mechanism. The pmf homeostasis in bacteria under various growth conditions also reflects the accommodation of pH homeostasis (39), and YqjA has also been previously shown to be necessary for adaptation to alkaline pH (19). Consistent with this hypothesis, we show that exposure of BC202 to a growth medium of pH 6.0 rescues its temperature sensitivity and cell division defects, possibly by reinforcing the pmf with an enhanced proton gradient and lowering the cytoplasmic pH. We also isolated a suppressor of BC202 temperature sensitivity—MdfA, a multidrug transporter of the major facilitator superfamily (MFS)—which exhibits transport promiscuity to a broad range of substrates and participates in pmf homeostasis and adaptation to alkaline conditions by acting as a Na^+/K^+-H^+ antiporter (40–43). In light of these results, we propose that YqjA and YghB play critical roles in envelope quality control and maintenance, possibly through homeostasis of pmf under a variety of growth conditions.

MATERIALS AND METHODS

Tryptone and yeast extract were from BD (Sparks, MD). Radioisotopes were purchased from PerkinElmer. Phusion/*Taq* polymerase, T4 DNA ligase, and all restriction enzymes were purchased from New England BioLabs. All other chemicals were reagent grade and purchased from either Sigma-Aldrich or VWR. *E. coli* was grown in Miller's LB broth (1% tryptone, 0.5% yeast extract, and 1% NaCl) unless otherwise mentioned. LB medium of pH 6.0 was buffered with 100 mM 2-(*N*-morpholino) ethanesulfonic acid (MES), and LB medium of pH 8.5 was buffered with 100 mM phosphate buffer. Ampicillin (Amp) (100 μg/ml), tetracycline (Tet) (12.5 μg/ml), kanamycin (Kan) (30 μg/ml), or chloramphenicol (Cam) (30 μg/ml) was added to the growth medium as necessary.

Construction of plasmids. pRS101. The *E. coli lacZ* gene was amplified from W3110 genomic DNA and placed behind the σ^{32}-regulated *grpE* promoter (81 bp upstream of *grpE*) (44) using forward primer *pRS101fp* and reverse primer *pRS101rp* (see Table S1 in the supplemental material). The PCR product was purified using the QIAquick PCR purification kit (Qiagen, Valencia, CA), digested with SalI and BamHI, and cloned into a similarly treated and dephosphorylated pACYC184 vector (NEB), yielding pRS101 (Table 1). Sequencing of all constructs was performed with an ABI 3130XL DNA sequencer in the Genomics Laboratory of Louisiana State University.

pRS102. *E. coli lacZYA* was amplified from W3110 genomic DNA so as to be under the control of the σ^E-regulated *degP* promoter (72 bp upstream of *degP*) (18) using forward primer *pRS102fp* and reverse primer *pRS102rp* (see Table S1 in the supplemental material). DNA was treated

TABLE 1 Bacterial strains and plasmids

Strain or plasmid	Relevant genotype/genetic markers	Source or reference
E. coli strains		
W3110	Wild type, F^- λ^-	*E. coli* Genetic Stock Center, Yale University
W3110F	W3110, Δ*pspF739*::Kan^r	This work
BC202	W3110, Δ*yqjA*::Tet^r Δ*yghB781*::Kan^r	4
BC203	W3110, Δ*yqjA*::Tet^r	4
BC204	W3110, Δ*yghB781*::Kan^r	4
BC202C	W3110, Δ*yqjA*::Tet^r Δ*cpxR772* Δ*yghB781*::Kan^r	This work
BC202F	W3110, Δ*yqjA*::Tet^r Δ*pspF739* Δ*yghB*781::Kan^r	This work
BC202R	W3110, Δ*yqjA*::Tet^r Δ*rcsB770* Δ*yghB*781::Kan^r	This work
BC202bae	W3110, Δ*yqjA*::Tet^r Δ*baeR778* Δ*yghB*781::Kan^r	This work
JW2976	F^- Δ*(araD-araB)567* Δ*lacZ4787(::rrnB-3)* λ^- Δ*yghB781*::Kan^r *rph-1* Δ*(rhaD-rhaB)568 hsdR514*	3
JW3883	F^- Δ*(araD-araB)567* Δ*lacZ4787(::rrnB-3)* λ^- *rph-1* Δ*(rhaD-rhaB)568* Δ*cpxR772*::Kan^r *hsdR514*	3
JW1296	F^- Δ*(araD-araB)567* Δ*pspF739*::Kan^r Δ*lacZ4787(::rrnB-3)* λ^- *rph-1* Δ*(rhaD-rhaB)568 hsdR514*	3
JW2205	F^- Δ*(araD-araB)567* Δ*lacZ4787(::rrnB-3)* λ^- Δ*rcsB770*::Kan^r *rph-1* Δ*(rhaD-rhaB)568 hsdR514*	3
JW0192	F^- Δ*(araD-araB)567* Δ*rcsF721*::Kan^r Δ*lacZ4787(::rrnB-3)* λ^- *rph-1* Δ*(rhaD-rhaB)568 hsdR514*	3
JW2064	F^- Δ*(araD-araB)567* Δ*lacZ4787(::rrnB-3)* λ^- Δ*baeR778*::Kan^r *rph-1* Δ*(rhaD-rhaB)568 hsdR514*	3
TB28	MG1655, Δ*lacIZYA*	45
RS28A	TB28, Δ*yqjA*::Tet^r	This work
RS28B	TB28, Δ*yghB*781::Kan^r	This work
RS28B*	TB28, Δ*yghB*781	This work
RS28C	TB28, Δ*cpxR772*::Kan^r	This work
RS28F	TB28, Δ*pspF739*::Kan^r	This work
RS28R	TB28, Δ*rcsB770*::Kan^r	This work
RS28bae	TB28, Δ*baeR778*::Kan^r	This work
RS28AB	TB28, Δ*yqjA*::Tet^r Δ*yghB*781::Kan^r	This work
RS28ABC	TB28, Δ*yqjA*::Tet^r Δ*cpxR772*::Kan^r Δ*yghB781*	This work
RS28ABF	TB28, Δ*yqjA*::Tet^r Δ*pspF739*::Kan^r Δ*yghB781*	This work
RS28ABR	TB28, Δ*yqjA*::Tet^r Δ*rcsB770*::Kan^r Δ*yghB781*	This work
RS28ABrcsF	TB28, Δ*yqjA*::Tet^r Δ*rcsF721*::Kan^r Δ*yghB781*	This work
RS28ABbae	TB28, Δ*yqjA*::Tet^r Δ*baeR778*::Kan^r Δ*yghB781*	This work
MVA4	MC1061 ϕ(*pspA-lacZ*) (Amp^r)	46
RSP28	TB28 ϕ(*pspA-lacZ*) (Amp^r)	This work
RSP28A	RS28A ϕ(*pspA-lacZ*) (Amp^r)	This work
RSP28B	RS28B ϕ(*pspA-lacZ*) (Amp^r)	This work
RSP28F	RS28F ϕ(*pspA-lacZ*) (Amp^r)	This work
RSP28AB	RS28AB ϕ(*pspA-lacZ*) (Amp^r)	This work
RSP28ABF	RS28ABF ϕ(*pspA-lacZ*) (Amp^r)	This work
TB28sc	TB28; pSH10; pRSpssAC	This work
RS28ABsc	RS28AB; pSH10; pRSpssAC	This work
Plasmids		
pBADHisA	Expression vector; *araBAD* promoter, Amp^r	Invitrogen
pBADCamHisA	Expression vector; *araBAD* promoter, Amp^r Cam^r	This work
pACYC184	Low-copy-number expression vector; Tet^r Kan^r	New England Biolabs
pRSpssAC	H_6-*pssA* expression vector; *araBAD* promoter, Amp^r	This work
pRS101	σ^{32}-responsive vector; Cam^r, pACYC184 (*grpE* promoter-*lacZ*)	This work
pRS102	σ^E-responsive vector; Cam^r, pACYC184 (*degP* promoter-*lacZ*)	This work
pRS103	RcsB-responsive vector; Cam^r, pACYC184 (*rprA* promoter-*lacZ*)	This work
pRS104	BaeR-responsive vector; Cam^r, pACYC184 (*mdtA* promoter-*lacZ*)	This work
pBADYqjA	H_6-*yqjA* expression vector; *araBAD* promoter, Amp^r	7
pBADMdfA	H_6-*mdfA* expression vector; *araBAD* promoter, Amp^r	This work
pBADTatABC	*tatABC* operon expression vector; *araBAD* promoter, Amp^r	5
pSH10	CpxR-responsive vector; Amp^r, pFZY1 (*cpxP* promoter-*lacZ*)	47
pCP20	FLP^+, λ cI857$^+$, λ ρ_R Rep^{ts} Amp^r Cam^r	48

with SalI and BamHI and ligated into a similarly treated and dephosphorylated vector, pACYC184, yielding pRS102 (Table 1).

pRS103. *E. coli lacZ* was amplified from W3110 genomic DNA so as to be under the control of the *rprA* promoter (56 bp upstream of *rprA*) (34) using forward primer *pRS103fp* and reverse primer *pRS101rp* (see Table S1 in the supplemental material). DNA was treated with SalI and BamHI and ligated into a similarly treated and dephosphorylated vector, pACYC184, yielding pRS103 (Table 1).

pRS104. We utilized a unique SpeI restriction site 40 bp upstream of the *mdtA* gene to create vector pRS104. *E. coli lacZ* was amplified from

W3110 genomic DNA using forward primer *pRS104fp1* and reverse primer *pRS101rp* (see Table S1 in the supplemental material) so that part of the *mdtA* promoter region (46 bp upstream of *mdtA*, including the SpeI site from −46 to −41) is present ahead of *lacZ*. DNA was treated with SalI and BamHI and ligated into a similarly treated and dephosphorylated vector, pACYC184, to yield an intermediate cloning vector, pRS104inc. The −321 to −47 region of the *mdtA* promoter was amplified from W3110 genomic DNA using forward primer *pRS104fp2* and reverse primer *pRS104rp* (see Table S1), treated with SalI and SpeI, and ligated into a similarly treated and dephosphorylated vector, pRS104inc, to yield pRS104, which contains the 321-bp promoter region of *mdtA* (37) fused to *lacZ*.

pBADMdfA. The *mdfA* gene was amplified from W3110 genomic DNA using primers *pBADMdfAfp* and *pBADMdfArp* (see Table S1 in the supplemental material). The PCR product was purified and digested with XhoI and HindIII and then ligated to a similarly digested and dephosphorylated pBADhisA (Invitrogen) vector. This resulted in the expression of MdfA from an arabinose-inducible promoter with an N-terminal hexahistidine tag.

pBADCamHisA. The *cat* (Cam^r) gene was amplified from a pPCR-Script-Cam (Stratagene) template using primers *CATfp* and *CATrp* (see Table S1 in the supplemental material). The PCR product was purified as for pBADMdfA, digested with SphI and AccI, and cloned into a similarly treated and dephosphorylated pBADHisA vector, resulting in pBADCam-HisA (Table 1), which confers resistance to both Cam and Amp. It retains all the cloning and expression properties of the pBADHisA vector.

pRSpssAC. The *E. coli pssA* gene was amplified from W3110 genomic DNA using primer sets *pRSpssAfp* and *pRSpssArp* (see Table S1 in the supplemental material). The PCR products were purified as before, digested with XhoI and HindIII, and cloned into a similarly treated and dephosphorylated pBADCam-HisA vector (Table 1). This resulted in the expression of the *E. coli pssA* gene with an N-terminal hexahistidine tag from an arabinose-inducible promoter, leading to the formation of plasmid pRSpssAC (Table 1).

Construction of strains. All strains and constructions were verified using colony PCR with primers flanking the relevant genes. In order to cure the Kan^r cassette, the temperature-sensitive plasmid pCP20 expressing FLP recombinase was used as described previously (48, 49). All strains and genotypes are listed in Table 1.

RS28A, RS28B, RS28C, RS28F, RS28R, RS28bae, and RS28AB (Table 1). Strain TB28 (45) was used to provide a Δ*lacZYA* background for certain strains. RS28A resulted from P1 transduction of Δ*yqjA*::Tet^r into strain TB28. RS28B was prepared by P1 transduction of Δ*yghB*781::Kan^r into TB28. Similarly, RS28C, RS28F, RS28R, and RS28bae were created by P1 transduction of Δ*cpxR772*::Kan^r, Δ*pspF739*::Kan^r, Δ*rcsB770*::Kan^r, and Δ*baeR778*::Kan^r, respectively, into TB28. RS28AB was generated by P1 transduction of Δ*yqjA*::Tet^r into strain RS28B.

RS28ABC, RS28ABF, RS28ABR, RS28ABrcsF, and RS28ABbae (Table 1). RS28ABC was generated starting from RS28B. The removal of the Kan^r cassette from RS28B with FLP recombinase expressed from pCP20 resulted in strain RS28B*. P1 transduction of Δ*cpxR772*::Kan^r into RS28B* resulted in generation of strain RS28BC. Subsequent P1 transduction of Δ*yqjA*::Tet^r into RS28BC resulted in strain RS28ABC. Similarly, RS28ABF, RS28ABR, RS28ABrcsF, and RS28ABbae were generated from P1 transduction of Δ*pspF739*::Kan^r, Δ*rcsB770*::Kan^r, Δ*rcsF721*::Kan^r, and Δ*baeR778*::Kan^r, respectively, into RS28B*, followed by subsequent P1 transduction of Δ*yqjA*::Tet^r into each of the resulting strains.

BC202C, BC202F, BC202R, and BC202bae. BC203 (4) was transduced to Kan^r using a P1 lysate from strain JW3883 (Table 1), and an isolate was subsequently cured of Kan^r using FLP recombinase, resulting in strain BC203C. Subsequent P1 transduction of Δ*yghB*781::Kan^r into strain BC203C resulted in strain BC202C. Following a similar procedure, Δ*pspF739*::Kan^r, Δ*rcsB770*::Kan^r, and Δ*baeR778*::Kan^r were transduced into BC203, followed by curing of Kan^r from each of the resultant strains using FLP recombinase, and subsequent P1 transduction of Δ*yghB*781::Kan^r into each of those cured strains resulted in strains BC202F, BC202R, and BC202bae, respectively.

RSP28, RSP28A, RSP28B, RSP28F, RSP28AB, and RSP28ABF (Table 1). RSP28, RSP28A, RSP28B, RSP28F, RSP28AB, and RSP28ABF were constructed by transducing strains TB28, RS28A, RS28B, RS28F, RS28AB, and RS28ABF, respectively, to Amp^r using a P1 lysate from strain MVA4 (46).

TB28sc and RS28ABsc. Plasmid pSH10 (Table 1) was transformed into strains TB28 and RS28AB, followed by a subsequent transformation with plasmid pRSpssAC, resulting in strains TB28sc and RS28ABsc (Table 1). Plasmid compatibility was ascertained by the ability of TB28sc to produce elevated levels of PE when grown in the presence of 0.2% arabinose as well as the capability of β-galactosidase production when challenged with alkaline growth conditions (data not shown).

β-Galactosidase assay. The β-galactosidase (β-gal) assays were carried out using the method of Miller (50). Overnight cultures of indicated strains containing plasmid pRS101, pRS102, pRS103, pRS104, or pSH10, or the RSP strains (Table 1), were diluted 1:100 in fresh LB medium supplemented with appropriate antibiotics and grown at 30°C and 225 rpm until they reached an optical density at 600 nm (OD_{600}) of ~1.0. The cultures were then diluted 1:3 in fresh LB medium, supplemented with appropriate antibiotics and additives, prewarmed to either 30°C or 44°C, and grown for the indicated times. Cells were harvested during exponential phase (OD_{600}, ~0.4 to 0.8); 50, 100, or 500 μl of cells was added to Z buffer (50) to a total volume of 1 ml, and the cells were lysed by the addition of 50 μl chloroform and 25 μl 0.1% SDS and vortexing. The reaction was started by the addition of 0.1 ml of 8 mg/ml (wt/vol) *o*-nitrophenyl-β-D-galactopyranoside (ONPG), and the tubes were incubated at 30°C until sufficient yellow color had developed (reaction time varied from 15 min to 4 h). The reaction was stopped by adding 0.4 ml of 1.25 M Na_2CO_3 to the reaction mix and vortexing. The mixture was centrifuged at 13,000 rpm for 10 min to remove cell debris, and absorbance was read at 420 nm. Cells harboring the empty vector gave a reading at 420 nm that was not above background. Units of β-galactosidase were corrected for culture density and correspond to 1 nmol ONPG hydrolyzed per minute at 30°C.

Determination of membrane potential (Δψ) using deconvolution fluorescence microscopy. The membrane potential (Δψ) was determined using a modified version of a previously described protocol (25, 46) employing the JC-1 red/green dye-based assay. JC-1 (Life Technologies) was prepared as a stock of 5 mg/ml in dimethyl sulfoxide (DMSO) and stored at −20°C until use. The working solution of the dye was prepared by first diluting 4 μl of the stock into 16 μl of DMSO, followed by a stepwise addition of 1 ml of a permeabilization buffer (25) containing 10 mM Tris, pH 7.5, 1 mM EDTA, and 10 mM glucose. Overnight cultures were diluted 1:100 in fresh LB medium with appropriate antibiotics and indicated additives. A 2-ml sample of the culture was harvested during exponential phase (OD_{600}, ~0.8), pelleted and resuspended in 1 ml working solution of JC-1, and subsequently incubated at 30°C in the dark. After incubation, 10 μl of cells was spotted on a 1% agarose-coated slide and immediately observed under a Leica DM-RXA2 deconvolution microscope. Green fluorescent protein (GFP) and tetramethyl rhodamine isocyanate (TRITC) filter sets were used for recording the green (530 nm) and the red (590 nm) emissions, respectively. Slidebook software (Intelligent Imaging Innovation, Denver, CO) was used to calculate the green/red fluorescence ratio from 100 cell units (individual cells or chains of cells) from 3 different experiments.

Microscopy. All microscopy was done with a Leica DM-RXA2 deconvolution microscope. All observations were recorded using a 100×, 1.30-numerical-aperture oil immersion objective lens. Images from the deconvolution microscope were captured through a DIC (differential interference contrast) filter by a cooled Cooke SensiCamQE 12-bit, 1.3-megapixel, charge-coupled-device digital camera and recorded using a workstation computer running Slidebook software. Overnight cultures of the indicated *E. coli* strains were diluted 1:100 in fresh LB medium with appropriate antibiotics and ad-

ditives and grown at 30°C in a shaking incubator. Live cells were harvested directly from the medium when the cultures reached midexponential phase (OD_{600}, ~0.6) by centrifugation and resuspended at a final OD_{600} of 1.0 in LB medium, and 10 μl was spotted on a 1% agarose-coated glass slide for imaging.

Membrane preparation and Western blotting. Membrane fractions were prepared from exponentially growing cultures of BC202 harboring pBADMdfA, which were either uninduced or induced with 0.02% arabinose or 0.2% arabinose, using a previously published protocol (51). Membranes were incubated in 3× SDS-PAGE buffer at room temperature for 20 min and subjected to SDS-PAGE. Western blotting was done by using Penta-His primary antibody (Qiagen) (1:5,000) and goat-anti-mouse horseradish peroxidase (HRP) secondary antibody (Pierce) (1:10,000). Detection was done with an ImmunStar HRP kit (Bio-Rad).

RESULTS

The σ^{32} cytoplasmic stress response pathway remains uninduced in BC202, while the σ^{E} periplasmic stress response pathway is repressed. We previously hypothesized that YqjA and YghB play critical roles in envelope quality control (5) and demonstrated that the DedA protein family is essential to both *E. coli* (7) and *B. burgdorferi* (9). The phenotypes of BC202 are similar to those of *E. coli* strains which are deficient in or which exhibit constitutive activation of certain stress response pathways (32, 52–54). It has also been previously reported that the Δ*yqjA E. coli* mutant exhibits an induction of the Cpx stress response and is sensitive to alkaline pH (19) and *yqjA* itself is subject to transcriptional regulation by both Cpx (19) and σ^{E} (18). Therefore, we measured the activation of various well-known stress response pathways in an *E. coli* Δ*yqjA* Δ*yghB* double mutant to better understand the physiological roles of these proteins.

We started with a Δ*lacZYA* parent strain, TB28 (45), and created the individual Δ*yqjA* and Δ*yghB* strains (RS28A and RS28B, respectively) as well as the Δ*yqjA* Δ*yghB* double mutant RS28AB (Table 1). As expected, the phenotypes of RS28AB are identical to those of BC202 (4, 5), as it exhibits inefficient cell division and fails to grow at temperatures above 42°C (data not shown). Therefore, RS28AB and BC202 were used interchangeably depending upon the requirements of individual experiments. In order to measure the activation of σ^{32} cytoplasmic stress response in all TB28 strains, we constructed plasmid pRS101 (Table 1), in which the expression of *lacZ* is under the control of a σ^{32}-regulated *grpE* promoter (44). The cytoplasmic stress response pathway is activated at elevated growth temperatures (55) and TB28 cultures shifted to 44°C for 30 min exhibit approximately 2-fold induction of β-galactosidase activity. Neither of the single-mutant strains RS28A and RS28B nor the RS28AB double mutant exhibit a significant increase in β-galactosidase activity compared to the parent strain at 30°C, indicating that the σ^{32} pathway is not activated under these conditions (Fig. 1A).

The induction of the σ^{E} periplasmic stress response was measured using plasmid pRS102 (Table 1), in which expression of *lacZ* is under the control of the *degP* promoter (18). TB28 cultures shifted to 44°C exhibit an approximately 2.4-fold induction of the σ^{E} stress response pathway (Fig. 1B), consistent with previous reports that this pathway is induced by heat stress (56, 57). RS28AB exhibits a minimal 1.2-fold induction of the σ^{E} stress response at 30°C compared to the parent TB28. It has been previously reported that the *E. coli degP* gene is under the regulation of both Cpx and σ^{E} stress response pathways (16, 19, 58). However, we have verified that our *degP* promoter-*lacZ* construct responds only to σ^{E} induction, as strains RS28AB and RS28ABC (Δ*yghB* Δ*yqjA* Δ*cpxR*) display similar degrees of σ^{E} induction (Fig. 1B). None of the remaining TB28-derived strains exhibit any significant activation of the σ^{E} response at 30°C. The activation of the σ^{E} stress response system is essential for bacterial survival at elevated growth temperatures (52). We show that RS28AB is capable of activating the σ^{E} stress response at higher growth temperatures, but this activation is repressed by its activated Cpx stress response (see below), since RS28ABC exhibits σ^{E} activation comparable to that of the parent strain at elevated growth temperatures (see Fig. S1 in the supplemental material). This is in accordance with previously published observations that σ^{E} and Cpx have partially overlapping regulons (16) and regulate the expression of the same periplasmic chaperones/proteases (e.g., DegP) (58) necessary for survival at elevated growth temperatures (59, 60). Taken together, these observations demonstrate that the σ^{E} stress response in BC202 is repressed by its Cpx activation and the σ^{32} cytoplasmic stress response remains uninduced under normal growth conditions.

The Cpx stress response pathway is strongly activated in BC202 under permissive growth conditions. The induction of the Cpx envelope stress response in TB28 and its mutants was measured using plasmid pSH10 (47), in which the CpxR-regulated promoter of *cpxP* is fused to *lacZ*, resulting in Cpx-dependent *lacZ* expression. The Δ*yqjA* strain RS28A exhibits an approximately 2-fold increase in the induction of the Cpx stress response compared to the parent TB28 (Fig. 1C), in agreement with previously published observations (19). The Δ*yghB* mutant RS28B does not induce Cpx-dependent transcription of *lacZ*. RS28AB (Δ*yqjA* Δ*yghB*), on the other hand, induces the Cpx pathway about 4.2-fold over control. This degree of induction is similar to previously published observations in a strain harboring the *cpxA24** mutation (47), which results in constitutive activation of the pathway. Deletion of *cpxR* (strains RS28C and RS28ABC) results in loss of Cpx induction (Fig. 1C). Challenging the parent strain TB28 with alkaline medium (pH 8.5) or with 5% ethanol (vol/vol) in the growth medium results in a 3-fold or a 2-fold induction, respectively, of the Cpx stress response. Both of these conditions can induce the Cpx stress response pathway in *E. coli* (14, 17, 61) and serve as positive controls for Cpx induction in our experiment.

Previous observations from other laboratories have shown that cell division defects arise due to constitutive activation of the Cpx pathway in *E. coli* (53). Therefore, we wished to determine the cause and effect of Cpx activation in BC202 and determine if it results from and/or causes any or all of the phenotypes exhibited by BC202. Deletion of *cpxR* in BC202 (strain BC202C) or RS28AB (strain RS28ABC) still results in strains with temperature sensitivity (Fig. 2A) and altered cell division (Fig. 2H). Therefore, we conclude that the activation of the Cpx pathway in BC202 is not the cause of any of these phenotypes. To determine if the Cpx activation in BC202 is the result of any of its phenotypes, we measured Cpx activation in RS28AB in the presence of 10 mM $MgCl_2$ or 400 mM NaCl, both of which correct the cell division (Fig. 2F and G) and temperature sensitivity (Fig. 2B and C) of BC202. We observed that the level of Cpx activation in RS28AB is attenuated by approximately 2.0- to 2.3-fold when grown in the presence of 10 mM Mg^{2+} or 400 mM NaCl but still remains activated 2-fold over that of the parent strain grown under similar conditions (see Fig. S2A in the supplemental material). This observation suggests that the factors which lead to both the cell division defects and

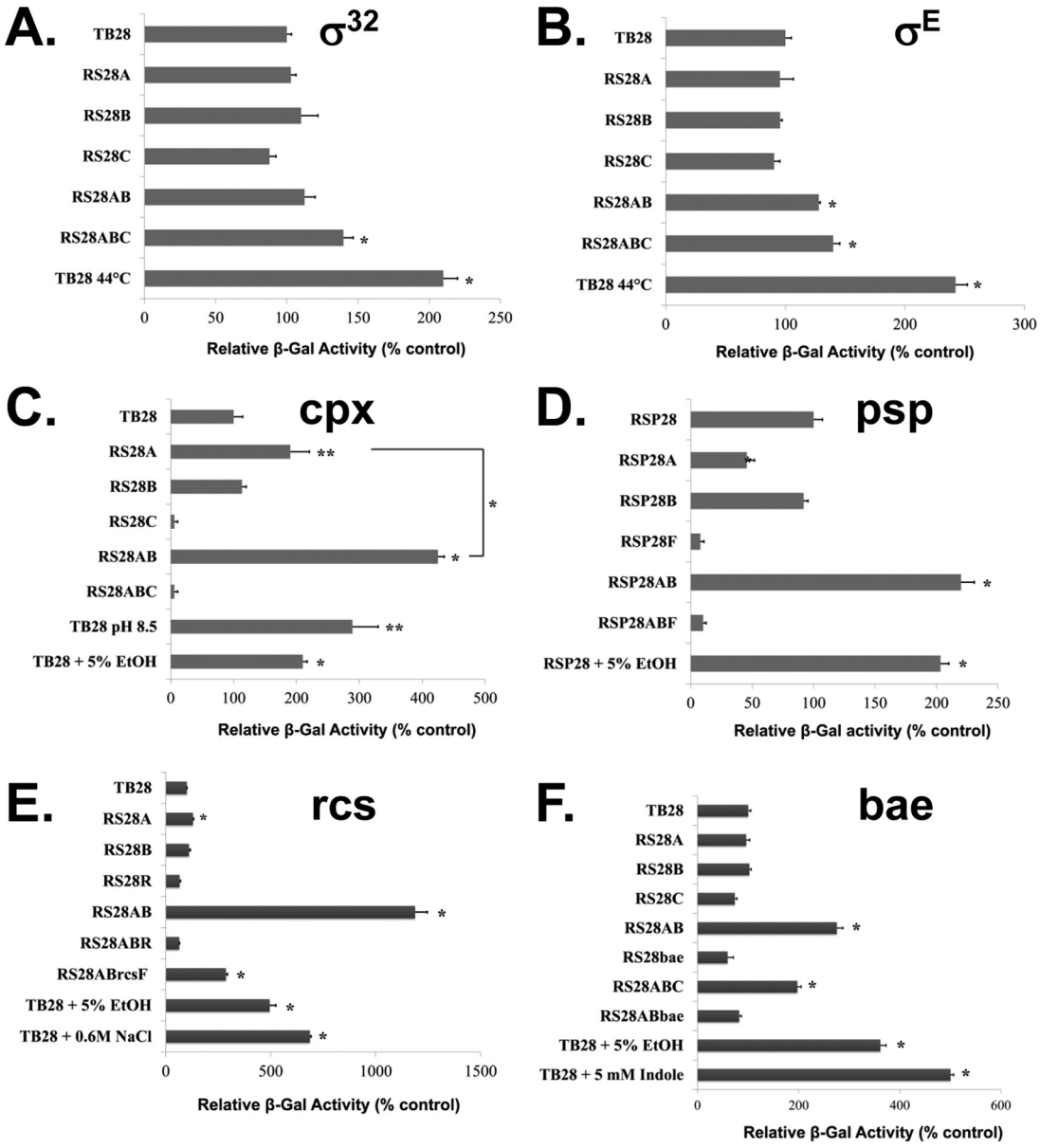

FIG 1 Activation of stress response pathways. The indicated strains were transformed with plasmid pRS101 (A), pRS102 (B) pSH10 (C), pRS103 (E), or pRS104 (F) to measure induction of σ^{32}, σ^{E}, Cpx, Rcs, and Bae pathways, respectively. The induction of Psp stress response was determined by using RSP strains (Table 1) containing the ϕ(pspA-lacZ) (Amp^r) chromosomal fusion (D). Cells were grown to exponential phase at 30°C unless otherwise indicated and assayed for β-galactosidase activity. Growth of TB28 at a higher temperature (44°C) for 30 min served as a positive control for induction of σ^{32} (A) and σ^{E} (B) stress responses. Growth of TB28 in alkaline medium (LB medium buffered with 100 mM phosphate buffer at pH 8.5) or in LB supplemented with 5% ethanol (EtOH) for 40 min served as a positive control for Cpx induction (C). Growth of RSP28 in LB supplemented with 5% EtOH for 30 min served as a positive control for activation of the Psp stress response (D). Growth of TB28 in LB supplemented with either 0.6 M NaCl or 5% EtOH for 45 min served as a positive control for Rcs activation (E). Growth of TB28 in LB supplemented with either 5 mM indole or 5% EtOH for 1 h served as a positive control for Bae activation (F). β-Galactosidase activity is expressed as a percentage of that displayed by the control parent strain, TB28. Each bar represents the average and standard deviation of three replicates of a representative experiment. Statistical significance was determined by Student's unpaired *t* test. The significance values are represented as follows: *, $P < 0.001$; **, $P < 0.01$.

temperature sensitivity in BC202 contribute only partially toward its increased Cpx activation, as both these defects can be corrected without fully alleviating the Cpx stress response in BC202. This is also supported by the observation that the *E. coli* Δ*yqjA* mutant does not share the growth and cell division phenotypes exhibited by BC202 (4) yet the Cpx stress response pathway remains activated. Therefore, we conclude that the Cpx pathway is not indirectly activated in BC202 as a result of its inefficient cell division and temperature sensitivity. In addition, we demonstrate (see Fig. S2B and C in the supplemental material) that the altered phospholipid composition of the Δ*yqjA* Δ*yghB* double mutant is not the cause of its Cpx activation, an observation made in a phosphatidylethanolamine-deficient strain (62).

BC202C (Δ*yqjA* Δ*yghB* Δ*cpxR*) not only retains all the pheno-

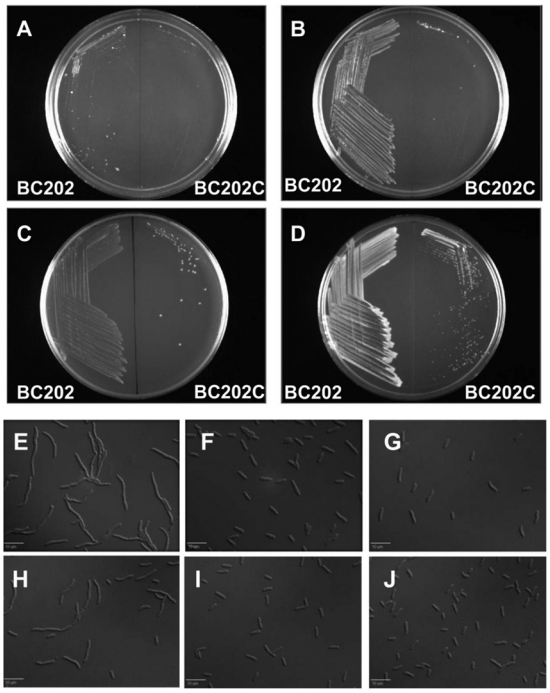

FIG 2 Cell division and temperature sensitivity of strains BC202 and BC202C under different growth conditions. Strains BC202 and BC202C (Table 1) were streaked onto LB agar plates (A) or LB agar plates supplemented with 10 mM $MgCl_2$ (B) or 400 mM NaCl (C). Alternatively, BC202 and BC202C were first transformed with plasmid pBADTatABC (5) and streaked on LB-Amp plates supplemented with 0.1% arabinose (D). All plates were incubated at 43°C overnight. Strains BC202 (E to G) and BC202C (H to J) were grown at 30°C to mid-log phase in LB medium (E and H) or LB medium supplemented with 10 mM $MgCl_2$ (F and I) or 400 mM NaCl (G and J). Cells were visualized with a Leica DM-RXA2 deconvolution microscope. Similarly, expression of TatABC partially restores cell division to BC202C (not shown), as was reported for BC202 (5).

types of BC202 but also exhibits additional prominent phenotypes. Unlike BC202, inclusion of either 10 mM $MgCl_2$ (Fig. 2B) or 400 mM NaCl (Fig. 2C) in the growth medium or overexpression of TatABC (Fig. 2D) fails to rescue the growth of BC202C at 43°C. However, as with BC202 (Fig. 2E to G), both 10 mM $MgCl_2$ (Fig. 2I) and 400 mM NaCl (Fig. 2J) do correct the cell division defect (Fig. 2H) of BC202C. Therefore, the ability of these additives to rescue growth of BC202 is dependent upon an intact Cpx pathway. Additionally, BC202C exhibits mucoid colony morphology on LB agar plates at 30°C (data not shown). Possible reasons for this phenotype are discussed later.

The Psp stress response pathway is activated in BC202 under permissive growth conditions. The Psp stress response was measured in strains containing the chromosomal ϕ(*pspA-lacZ*) (Amp^r) fusion that are here designated RSP strains (Table 1). In these strains, the expression of *lacZ* is under the control of the PspF-regulated *pspA* promoter as described previously (25, 46). The Psp stress response pathway is strongly and transiently activated when challenged with conditions which impair inner membrane integrity, such as exposure to extreme heat shock (48 to 50°C) or 5 to 10% ethanol or growth in the presence of carbonyl cyanide *m*-chlorophenylhydrazone (CCCP), an ionophore which dissipates the pmf at the membrane (14, 25). As expected, strains RSP28F and RSP28ABF express little *lacZ* activity due to the absence of PspF (Fig. 1D). The parent strain RSP28 displays about 2-fold induction of the Psp stress response when challenged with 5% ethanol for 30 min, and this condition serves as a positive control for this experiment. Interestingly, the Δ*yqjA* strain RSP28A exhibits a reproducible 2-fold reduction of Psp stress response compared to the parent for reasons that are not clear (see Discussion). The Δ*yghB* strain shows no significant change in Psp response, while the Δ*yqjA*/Δ*yghB* strain RSP28AB exhibits approximately 2-fold induction of the Psp stress response compared to the parent strain (Fig. 1D), similar to levels seen when the parent strain RSP28 is challenged with 5% ethanol.

The activation of the Psp stress response has been previously associated with impaired protein translocation via both the Sec and Tat secretion systems, and increased expression of PspA was shown to stimulate both Sec- and Tat-mediated secretion (63–65). These results have been attributed to the capability of PspA to bind to the inner membrane and prevent proton leakage (28). It has also been shown that efficient Tat-mediated protein secretion relies on the pmf (66, 67). These observations prompted us to check if we could correlate the cell division defects and temperature sensitivity of BC202 with its elevated Psp stress response.

Strains BC202F and RS28ABF were constructed by deletion of *pspF* from strains BC202 and RS28AB, respectively (Table 1). Both RS28ABF (not shown) and BC202F (see Fig S5D in the supplemental material) retain the temperature sensitivity and cell division defects (data not shown) of their corresponding double mutants, suggesting that the Psp activation in BC202 is not the cause of these phenotypes. Additionally, strain RSP28AB, when grown in medium supplemented with 10 mM $MgCl_2$ or 400 mM NaCl to correct temperature sensitivity and cell division, displays a significant reduction in its Psp induction (see Fig. S3 in the supplemental material). Therefore, we conclude that the activation of Psp stress response in BC202 is independent of its cell division defects and temperature sensitivity but that the Psp stress response and the phenotype changes result from a common cause—compromised envelope integrity coupled with a loss of pmf.

The Rcs stress response pathway is strongly activated in BC202 in an RcsF-dependent manner. To measure the induction of Rcs stress response, we cloned *lacZ* under the control of the *rprA* promoter in vector pACYC184, yielding plasmid pRS103 (Table 1). RprA is a small regulatory RNA and is under the transcriptional control of RcsB (34). The Rcs pathway is strongly induced when *E. coli* cultures are exposed to 5% ethanol or 0.6 M NaCl (14), and both of these conditions serve as positive controls for Rcs activation in our experiment. Growing the parent strain TB28 harboring plasmid pRS103 in 5% ethanol or 0.6 M NaCl for 45 min caused about 5- and 7-fold activation, respectively, of the Rcs stress response (Fig. 1E). The Δ*yqjA* mutant RS28A exhibits a small but significant ($P < 0.01$) 1.3-fold activation of Rcs response over the parent strain. Surprisingly, RS28AB (Δ*yqjA* Δ*yghB*) displays an extremely strong (about 12-fold) induction of the Rcs stress response under permissive growth conditions, with activation levels similar to those found in constitutively active Δ*rcsC* mutants (32). This strong activation is partially dependent on the OM lipoprotein RcsF, because deletion of *rcsF* in RS28AB (strain RS28ABrcsF) led to about a 4-fold reduction of the Rcs stress response, but it still remains about 3-fold activated compared to the parent strain (Fig. 1D). Deletion of response regulator *rcsB* led to a decrease in β-gal activity of both the parent (strain RS28R) and the Δ*yqjA* Δ*yghB* double mutant (strain RS28ABR).

The strong Rcs activation in BC202 automatically raises the question of whether the temperature sensitivity of BC202, which results in cell lysis after about a 2-h growth at nonpermissive temperatures (4), is due to its strong Rcs activation. Therefore, we proceeded to check if the activation of Rcs phosphorelay in BC202 is related to its phenotypes. Both RS28ABR and BC202R retain the characteristic cell division defects (data not shown) and temperature sensitivity (BC202R [see Fig. S5Ei in the supplemental material]), even when the Rcs activation has been attenuated by the removal of the transcriptional response regulator RcsB (Fig. 1D). This suggests that Rcs activation in BC202 is not the cause of its cell division defects and temperature sensitivity. Growth of the strain RS28AB harboring pRS103 in LB medium supplemented with 10 mM $MgCl_2$ completely alleviates the Rcs stress response, while addition of 400 mM NaCl in growth medium or growth in acidic medium (pH 6.0) partially but significantly attenuates the Rcs response in RS28AB (see Fig. S4 in the supplemental material). All of these growth conditions can restore the cell division and temperature sensitivity of BC202/RS28AB (this study and reference 4). These results lead us to conclude that the cell division and temperature sensitivity of BC202 are unrelated to its Rcs activation and probably share a cause stemming from a perturbed envelope.

The Bae stress response is significantly activated in BC202. In order to measure the activation of the Bae stress response system, we cloned *lacZ* under regulation of the BaeR-responsive *mdtA* promoter in vector pACYC184, resulting in the plasmid pRS104 (Table 1). The promoter of *mdtA* is dependent on both CpxR and BaeR for optimal activation (37). Since the Cpx pathway is already induced in BC202, we verified that pRS104 responds to Cpx activation only. As shown in Fig. 1E, deletion of *cpxR* did lower the *mdtA* promoter activity in both TB28 and RS28AB (strains RS28C and RS28ABC, respectively) but RS28ABC still exhibits about 2-fold induction of the Bae stress response compared to TB28. This corresponds to previous reports that the *mdtABCD* operon either remains largely unaffected by several Cpx-activating conditions, such as CpxR overexpression or the presence of the constitutively activating *cpxA24** allele, or is even negatively regulated by conditions such as NlpE overexpression (19). The well-known activators of the Bae stress response in *E. coli* are indole and ethanol (14, 37). We used both of these conditions as positive controls in our experiment. Exposure of the parent strain TB28 to 5% ethanol and 5 mM indole for an hour resulted in a 3.6-fold and a 5-fold induction, respectively, of the Bae stress response (Fig. 1E). Deletion of *baeR* results in reduction of promoter activity in both the parent strain RS28bae and the Δ*yqjA* Δ*yghB* double mutant (strain RS28ABbae). RS28AB exhibits about a 2.8-fold activation of the Bae stress response pathway (Fig. 1E). Deletion of *baeR* in either RS28AB or BC202 results in strains RS28ABbae and BC202bae, respectively. Both these triple mutants retain the temperature sensitivity (BC202bae [see Fig. S5Ek in the supplemental material]) and cell division defects (data not shown) of their corresponding double mutants. Growth of the strain RS28AB harboring pRS104 in LB supplemented with 10 mM $MgCl_2$ or 400 mM NaCl or in acidic medium (pH 6.0) partially but significantly alleviated its Bae activation (see Fig. S6 in the supplemental material). All of these growth conditions can restore the cell division and temperature sensitivity of BC202/RS28AB (this study and reference 4). Taken together, these results suggest that, similar to the Cpx, Psp, and Rcs stress responses observed in BC202, Bae activation is also independent of its growth and cell division phenotypes and thus these actions share a cause—a perturbation in the envelope.

BC202 exhibits a significant loss of membrane potential. The proton motive force (pmf) in *E. coli* comprises two components—the transmembrane electrical membrane potential difference, $\Delta\psi$ ($= \psi_{in} - \psi_{out}$), with ψ_{in} (electrical potential inside) being more negative than ψ_{out} (electrical potential outside), and the transmembrane pH difference, ΔpH ($= pH_{in} - pH_{out}$), with pH_{in} (intracellular pH) being more alkaline than pH_{out} (extracellular pH) under normal growth conditions. This pattern varies due to physiological processes involved in pmf homeostasis when *E. coli* cells are subjected to adverse growth conditions like alkaline pH (39). Any alteration in one component of the pmf results in a simultaneous compensative change in the other which maintains an optimal pmf and nearly constant cytoplasmic pH (~7.6) over a diverse range of growth conditions (39).

It has been previously demonstrated (23, 26) that loss of envelope integrity leading to dissipation of pmf results in induction of the Psp stress response. Efficient Tat-mediated secretion of substrates also relies on optimal pmf (66–68). RS28AB exhibits about a 2-fold induction of the Psp stress response under normal growth conditions compared to parent TB28 (Fig. 1D), alongside a defect in cell division resulting from inefficient Tat-mediated secretion of periplasmic amidases AmiA and AmiC (5). Therefore, we measured the relative membrane potential of BC202 using a previously described protocol (23, 25) relying on the JC-1 red/green dye-based assay. JC-1 is a membrane-permeating dye which in its monomeric form emits a green fluorescence (~530 nm) when excited. It exhibits a potential-dependent accumulation at the bacterial membrane, causing formation of J aggregates whose fluorescence emission shifts from green to red (~590 nm). Consequently, we can express the membrane potential as a ratio of its red/green fluorescence intensities.

BC202 (Fig. 3B and D) exhibits a significant loss of membrane potential compared to W3110 (Fig. 3A and D). Treatment of W3110 with 100 μM CCCP for 20 min (Fig. 3C) also results in a loss of membrane potential, as indicated by its high green/red ratio (Fig. 3D). Since BC202 cells are mostly in chains of varied lengths, we considered a chain of cells as a single unit wherein we calculated its total red and green fluorescence intensities. BC202 chains containing lower numbers of cells per chain (<4) often exhibit a membrane potential which is comparable to that of the parent strain, but longer chains were often characterized by more green and minimal red regions. Deletion of PspF in the Δ*yqjA* Δ*yghB* strain results in loss of Psp induction (Fig. 1D), and subsequently there is a significant loss of membrane potential in BC202F compared to BC202 (Fig. 3D). The single-deletion mutants BC203 and BC204 demonstrate only a small loss of membrane potential. BC202 grown at a higher temperature of 44°C for 1 h exhibits a degree of membrane potential deficiency similar to that found when it is grown at 30°C. These results demonstrate that the induction of Psp stress response in BC202 is an effect of its loss of membrane potential under normal growth conditions. This deficiency in membrane potential is exacerbated when BC202 loses its ability to activate the Psp stress response.

The cell division defect and temperature sensitivity of BC202 can be rescued by either overexpression of MdfA or growth at pH 6.0. Isolation of multicopy suppressors of BC202 was done following a previously described protocol (69). Plasmids that re-

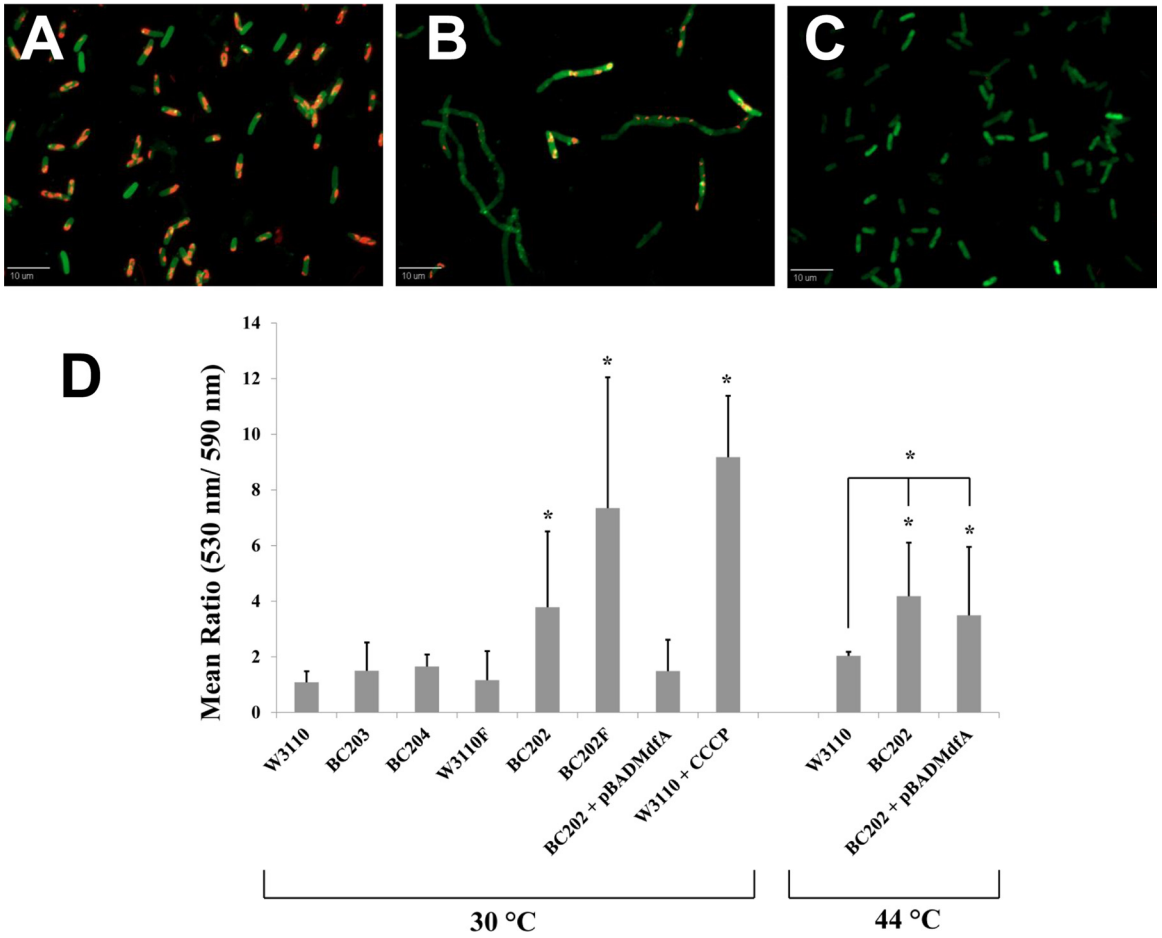

FIG 3 Assessment of the membrane potential ($\Delta\psi$) using JC-1 red/green dye-based assay. Strains W3110, W3110F, BC203, BC204, BC202, and BC202F transformed with empty vector pBADhisA and BC202 harboring plasmid pBADMdfA were grown in LB-Amp medium. BC202 harboring pBADMdfA was grown in the presence of 0.2% arabinose. W3110 treated with 100 μM CCCP for 20 min served as a control for loss of $\Delta\psi$. As indicated, strains were grown at either 30°C or 44°C. Membrane potential at higher growth temperatures was determined by growing strains W3110, BC202, and BC202 harboring pBADMdfA at 44°C for 1 h. All strains were treated with JC-1 dye in a permeabilization buffer as described in Materials and Methods and subjected to fluorescence deconvolution microscopy. The red and green intensities were captured using the TRITC (590 nm; exposure time, 300 ms) and the GFP (530 nm; exposure time, 1,500 ms) filter sets, respectively, and quantified using Slidebook software. (A to C) Fluorescent red-green overlay images of W3110 (A), BC202 (B), and W3110 treated with CCCP (C). (D) Changes in $\Delta\psi$ are presented as the green (530 nm)/red (590 nm) ratio. Each bar represents the mean and standard deviation of the ratio of total red and green intensities determined from 100 cell units (cells or chains) from three independent experiments. Statistical significance was determined by Student's unpaired *t* test. The significance values are represented as follows: *, $P < 0.001$; **, $P < 0.01$. An increase in the green/red ratio indicates a decrease in membrane potential ($\Delta\psi$).

stored the growth of BC202 at 42°C were isolated and sequenced. One of the sequenced inserts was found to contain 4 genes: *mdfA*, *ybjH*, *ybjI*, and *ybjJ*. We cloned *mdfA*, which encodes a multidrug transporter with Na^+/K^+-H^+ antiporter functions (42), with an N-terminal His tag under the regulation of an arabinose-inducible promoter (vector pBADMdfA) (Table 1). BC202 transformed with empty vector pBADhisA and BC202 transformed with vector pBADMdfA were grown in the absence (Fig. 4C) or presence (Fig. 4D) of 0.1% arabinose on LB-Amp plates overnight at 43°C. BC202 harboring empty vector pBADhisA failed to grow under either condition, whereas BC202 harboring vector pBADMdfA grew at 43°C only in the presence of 0.1% arabinose. In addition, normal cell division was restored to BC202 at 30°C when MdfA was overexpressed (Fig. 4B). This rescue of cell division was accompanied by an increase in the membrane potential when MdfA was overexpressed in BC202 at 30°C (Fig. 3D). Overexpression of H_6-MdfA from pBADMdfA in an arabinose-dependent manner is shown by Western blotting (Fig. 4E). MdfA overexpression also restored growth of strains BC202C (see Fig. S5Cf in the supplemental material), BC202F (see Fig. S5Fh in the supplemental material), BC202R (see Fig. S5Fj in the supplemental material), and BC202bae (see Fig. S5Fl in the supplemental material) at 43°C.

The inability to maintain optimal pmf at neutral pH can be overcome by growth under acidic conditions. Acidic pH reinforces/increases the pmf by providing an enhanced proton gradient (39) ($pH_{out} < pH_{in}$). Strains were grown in LB medium at pH 6.0 buffered with 100 mM MES. The Na^+ concentration in the buffered LB medium was made equivalent to that of normal LB growth medium (~170 mM). BC202 grown in LB medium of pH 6.0 displayed normal cell division (Fig. 5F) and growth at 43°C (Fig. 5B), unlike when it was grown in LB medium at pH 7.0 (Fig. 5A). A similar correction of phenotypes was observed when BC202C, BC202F, BC202R, and

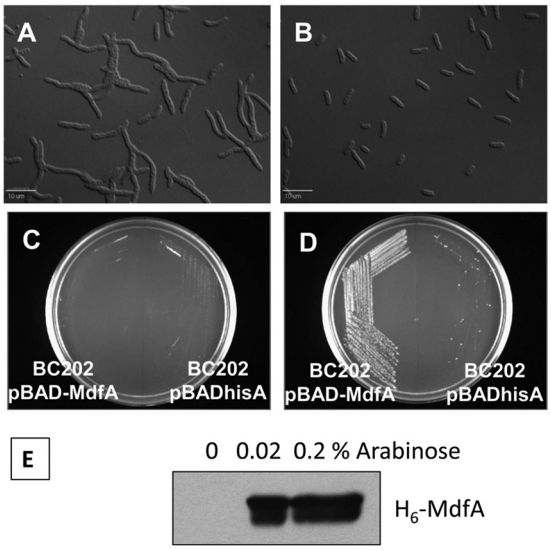

FIG 4 MdfA overexpression corrects the cell division defect and restores growth to BC202 at 43°C. (A and B) Normal cell division is restored to BC202 at 30°C in the presence of 0.2% arabinose (B) which induces MdfA expression from the plasmid. (C and D) BC202 harboring empty vector pBADhisA or vector pBADMdfA was streaked on LB-Amp-agar plates in the absence (C) or presence (D) of 0.1% arabinose and incubated overnight at 43°C. BC202 harboring pBADhisA (right sides of plates) fails to grow on either plate. BC202 harboring pBADMdfA (left sides of plates) grows only in the presence of 0.1% arabinose. (E) Western blot using anti-His tag antibody showing MdfA overexpression in BC202 from pBADMdfA in an arabinose-dependent manner. Equal amounts of membrane protein were loaded in each lane.

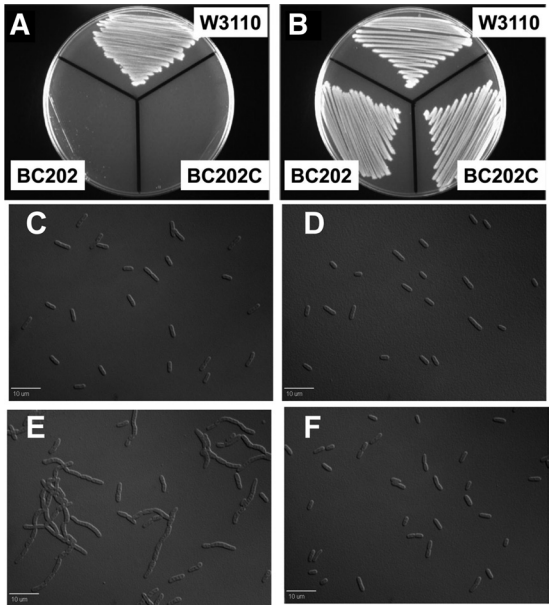

FIG 5 Rescue of cell division defect and temperature sensitivity of BC202 and BC202C in LB medium of pH 6.0. Strains W3110, BC202, and BC202C, harboring empty vector pBADhisA, were grown in LB-Amp medium at pH 7.0 and LB-Amp medium buffered with 100 mM MES at pH 6.0 at 30°C. The cell chaining of BC202 (E) observed in LB medium at pH 7.0 is corrected in LB medium at pH 6.0 (F). The cell division of W3110 (C and D) is unaltered in growth medium of either pH. The temperature sensitivity of BC202 and BC202C (A) observed on LB-agar plates at pH 7.0 at 43°C is rescued (B) when they are grown in LB-agar plates at pH 6.0 at 43°C.

BC202bae were grown in buffered LB medium at pH 6.0 (Fig. 5B and data not shown).

Taken together, these results demonstrate that MdfA is a potent suppressor of the cell division and temperature-sensitive phenotypes exhibited by BC202. Similar results can be observed with mild acidification of the growth medium. The commonality between these suppressors is that they enhance the proton influx across the inner membrane. These results strongly support the hypothesis that YqjA and YghB are required for proper pmf/pH homeostasis in *E. coli*.

DISCUSSION

The DedA family of membrane proteins is highly conserved and likely essential in many bacterial species (81). *E. coli* encodes as many as eight DedA family genes, and a distinct phenotype is not observed unless *yqjA* and *yghB* are simultaneously deleted (4). In this study, we analyzed the induction of several stress responses and discovered that the Cpx, Psp, Rcs, and Bae envelope responses are significantly activated in the Δ*yqjA* Δ*yghB* strains (BC202 and RS28AB) under permissive growth conditions (Fig. 1). These results strongly suggest that BC202 experiences significant envelope stress when grown under permissive conditions and that YghB/YqjA play critical roles in envelope homeostasis.

We were also interested in determining the effect of the induction of multiple envelope stress response pathways on the other observable phenotypes of BC202, namely, temperature sensitivity and altered cell division. We show that the induction of Cpx stress response is a distinct phenotype and is independent of the other major phenotypes exhibited by BC202. While deletion of *cpxR* from BC202 (strain BC202C) (Table 1) eliminates the activation of Cpx response, BC202C retains all of the phenotypes exhibited by BC202. In addition, growth of BC202C at 42°C is not rescued by the presence of millimolar concentrations of Mg^{2+} or 400 mM NaCl in growth medium (Fig. 2). Similarly, deletion of *pspF*, *rcsB*, and *baeR* from BC202 (strains BC202F, BC202R, and BC202bae, respectively) eliminates the activation of the Psp, Rcs, and Bae stress response pathways, respectively, in BC202. All of these strains retained the cell division and temperature sensitivity of BC202 and, unlike BC202C, were rescued by suppressors which are capable of rescuing the phenotypes of BC202, namely, growth in 10 mM Mg^{2+} or 400 mM Na^{+}.

In addition to the phenotypes mentioned above, BC202C exhibits a lower growth rate than BC202 and exhibits enhanced mucoid colony morphology on LB agar plates at 30°C (data not shown), unlike BC202. The colanic acid biosynthetic genes (cps) need to be upregulated for this phenotype, and such upregulation relies on both RcsB and RcsA (30). The *rprA* promoter-based reporter assay that we describe in this study relies only on RcsB. This observation can be explained in light of previously published data indicating that activation of Cpx upregulates the transcriptional regulator H-NS (14), which in turn represses the transcriptional levels of RcsA (70). Hence, BC202, which exhibits a strong induction of the Cpx stress response as well as the Rcs stress response, does not exhibit mucoid colony morphology. In the absence of *cpxR* in BC202C, it is possible that the H-NS levels are downregulated and consequently RcsA levels are elevated enough to allow enhanced colanic acid production and subsequent mucoid colony formation. Surprisingly, BC202F, BC202R, and BC202bae do not show any apparent additional phenotypes.

The induction of the Psp stress response in BC202 (Fig. 1D) is in agreement with our observation that the membrane potential is significantly lower in BC202 than in the parent strain (Fig. 3). The single Δ*yqjA* mutant, surprisingly, displays a >50% decrease in activity of the *pspA* promoter (Fig. 1D). Previous observations have demonstrated that in the absence of *cpxR*, the levels of PspF are increased 3-fold (14). This might indicate that the activation of Cpx stress response in the Δ*yqjA* mutant represses the PspF-dependent *pspA* promoter activity.

The Rcs pathway is strongly induced in BC202 (Fig. 1E), with activation similar to that found in constitutively active Δ*rcsC* mutants (32). The activation is at least partially dependent on RcsF, an outer membrane lipoprotein (36). The activation of the Rcs pathway is only poorly understood, and it has been reported activated in only a few strains, such as mutants of membrane-derived oligosaccharide glycosyltransferases (*mdoH*) (29) and those with alterations in lipoprotein transport and localization (71, 72), perturbations of the peptidoglycan layer (33), and changes in the phosphorylation levels of undecaprenyl carrier lipid (35). We can now add BC202 to this list. The Rcs pathway is necessary for RpoS-mediated acid and base resistance, and the small regulatory RNA RprA plays an important role in the translational regulation of RpoS (34, 73). It is difficult to say at this point if the Rcs stress response observed in BC202 is a result of its loss of pmf homeostasis, as we have proposed. It is possible that BC202 might try to prevent proton leakage and the induction of Psp stress response is not sufficient to downregulate nonvital processes like motility to conserve protons, so the Rcs pathway is called upon. Similarly to the Psp stress response (25, 26), the Rcs stress response has been reported to downregulate motility in the early stages of biofilm formation (30). In this regard, we have observed that BC202 is nonmotile (R. Sikdar and W. T. Doerrler, unpublished observations).

We also report a new multicopy suppressor for BC202 (Fig. 4)—the multidrug transporter MdfA, which plays a very important role in pmf homeostasis and mediates tolerance to alkaline conditions via an Na^+/K^+-H^+ antiport activity (42). Based on the characteristics of this suppressor, we hypothesize that the phenotypes of BC202 are the result of an impaired pmf homeostasis mechanism in BC202, which is inefficient at all growth temperatures. The activation of the Psp stress response and the loss of membrane potential in BC202 under normal growth conditions support this idea. Further evidence to support this hypothesis comes from the observation that lowering the pH of growth medium, which strengthens the pmf by providing an enhanced proton gradient (ΔpH) and promotes proton influx across the membrane, corrects the cell division and temperature sensitivity of BC202 (Fig. 5). We can explain the phenotype-rescuing capability of Mg^{2+} and Na^+ (4) on similar lines. Increasing Mg^{2+} levels can have multiple effects on bacterial cells—it can support/enhance membrane integrity in general and have specific effects like inhibiting the proton-extruding ATPase activity of the F_0F_1-ATP synthase machinery (74, 75). It is important to note that when bacterial cells are exposed to conditions which require proton influx into the cytoplasm, such as alkaline growth conditions, the expression of proton-pumping F_0F_1-ATP synthase is elevated in *E. coli* along with a repression of proton-extruding respiratory chain complexes (39). Monovalent cations like Na^+ can stimulate the activity of several classes of Na^+/K^+ proton antiporters, many of which have a central role in pH homeostasis under a variety of growth conditions (for example, NhaA [76, 77] and MdfA [42]). However, since both Mg^{2+} and Na^+ rely on Cpx activation to rescue the temperature sensitivity of BC202, it is possible that some Cpx-induced gene(s) is required for these conditions to rescue the growth defect of BC202. While the identity of this gene is not known, the list of Cpx-induced genes in *E. coli* is not exhaustively long (14, 19) and experiments are in progress to answer this question.

Based on the observations presented in this study, we propose that YqjA/YghB plays a role in pmf homeostasis. This is also in accordance with previously published observations (19) that YqjA is required for *E. coli* for adaptation to alkaline pH. YqjA/YghB can execute this role either directly as proton transporters or indirectly as regulators/modulators of an existing pH homeostasis mechanism. The idea that they may be a novel class of transporters with possible proton antiport functions similar to MdfA is indeed intriguing. Using NCBI BLAST, we could not find any amino acid similarity between YqjA/YghB and any existing class of transporters. However, evidence does exist which provides credence to this idea. The DedA protein family bears limited similarity to the LeuT family of transporters: they potentially share an ancestor, as revealed by a novel type of evolutionary analysis known as AlignMe (2). The DedA homolog of *Ralstonia metallidurans* has been implicated in selenite uptake by the bacterium (78). The *Mycobacterium* DedA homolog BCG2664 has been found to confer resistance to a macrocyclic alkaloid halicyclamine-A (79), and as is often the case with macrocyclic drugs, resistance is conferred by the action of several classes of multidrug transporters which help to secrete the drug outside the cell (80). These observations collectively support the idea that YqjA/YghB may belong to a novel family of membrane transporters.

Since MdfA overexpression rescues the temperature sensitivity of BC202, it is highly likely that the proton antiport (influx) function of MdfA is responsible for that observation. If we hypothesize that the pH_{in} of BC202 is more alkaline under normal growth conditions due to inefficient pH homeostasis, we can explain how overexpression of MdfA can rescue the phenotypes of BC202 by promoting proton influx and lowering the cytoplasmic pH. We can also explain the phenotype-rescuing capability of low-pH medium on similar lines. Growth in acidic pH can reinforce the pmf in BC202 by enhancing the ΔpH component, thus rescuing the cell division defect. Additionally, the enhanced proton gradient provided by acidic medium leads to increased proton influx across the inner membrane, which rescues the temperature sensitivity of BC202 by lowering the cytoplasmic pH. Acidification of the cytoplasm below the threshold is prevented by several mechanisms which participate in acid resistance (39). Both MdfA and lower external pH alleviate alkaline stress by enhancing proton influx across the inner membrane and consequently acidifying the cytoplasm. Further studies will test these ideas and try to pinpoint functions of the DedA membrane proteins.

ACKNOWLEDGMENTS

We thank Yoshinori Akiyama for kindly providing us with plasmid pSH10, Martin Buck for strain MVA4, Thomas Bernhardt for strain TB28, and anonymous reviewers for valuable suggestions and corrections. Thanks also go out to members of the Doerrler lab—Lisa Boughner and Sujeet Kumar—for critical reading of the manuscript.

Financial support has been provided by the National Science Foundation (MCB-0841853, to W.T.D.).

REFERENCES

1. **Elofsson A, von Heijne G.** 2007. Membrane protein structure: prediction vs reality. Annu. Rev. Biochem. **76**:125–140.
2. **Khafizov K, Staritzbichler R, Stamm M, Forrest LR.** 2010. A study of the evolution of inverted-topology repeats from LeuT-fold transporters using AlignMe. Biochemistry **49**:10702–10713.
3. **Baba T, Ara T, Hasegawa M, Takai Y, Okumura Y, Baba M, Datsenko KA, Tomita M, Wanner BL, Mori H.** 2006. Construction of Escherichia coli K-12 in-frame, single-gene knockout mutants: the Keio collection. Mol. Syst. Biol. **2**:2006.0008. doi:10.1038/msb4100050.
4. **Thompkins K, Chattopadhyay B, Xiao Y, Henk MC, Doerrler WT.** 2008. Temperature sensitivity and cell division defects in an Escherichia coli strain with mutations in yghB and yqjA, encoding related and conserved inner membrane proteins. J. Bacteriol. **190**:4489–4500.
5. **Sikdar R, Doerrler WT.** 2010. Inefficient Tat-dependent export of periplasmic amidases in an *Escherichia coli* strain with mutations in two DedA family genes. J. Bacteriol. **192**:807–818.
6. **Lee PA, Tullman-Ercek D, Georgiou G.** 2006. The bacterial twin-arginine translocation pathway. Annu. Rev. Microbiol. **60**:373–395.
7. **Boughner LA, Doerrler WT.** 2012. Multiple deletions reveal the essentiality of the DedA membrane protein family in Escherichia coli. Microbiology **158**(Pt 5):1162–1171.
8. **Fraser CM, Casjens S, Huang WM, Sutton GG, Clayton R, Lathigra R, White O, Ketchum KA, Dodson R, Hickey EK, Gwinn M, Dougherty B, Tomb JF, Fleischmann RD, Richardson D, Peterson J, Kerlavage AR, Quackenbush J, Salzberg S, Hanson M, van Vugt R, Palmer N, Adams MD, Gocayne J, Weidman J, Utterback T, Watthey L, McDonald L, Artiach P, Bowman C, Garland S, Fuji C, Cotton MD, Horst K, Roberts K, Hatch B, Smith HO, Venter JC.** 1997. Genomic sequence of a Lyme disease spirochaete, *Borrelia burgdorferi*. Nature **390**:580–586.
9. **Liang FT, Xu Q, Sikdar R, Xiao Y, Cox JS, Doerrler WT.** 2010. BB0250 of Borrelia burgdorferi is a conserved and essential inner membrane protein required for cell division. J. Bacteriol. **192**:6105–6115.
10. **Dilks K, Rose RW, Hartmann E, Pohlschroder M.** 2003. Prokaryotic utilization of the twin-arginine translocation pathway: a genomic survey. J. Bacteriol. **185**:1478–1483.
11. **Ize B, Stanley NR, Buchanan G, Palmer T.** 2003. Role of the Escherichia coli Tat pathway in outer membrane integrity. Mol. Microbiol. **48**:1183–1193.
12. **Sargent F, Bogsch EG, Stanley NR, Wexler M, Robinson C, Berks BC, Palmer T.** 1998. Overlapping functions of components of a bacterial Sec-independent protein export pathway. EMBO J. **17**:3640–3650.
13. **Stanley NR, Findlay K, Berks BC, Palmer T.** 2001. Escherichia coli strains blocked in Tat-dependent protein export exhibit pleiotropic defects in the cell envelope. J. Bacteriol. **183**:139–144.
14. **Bury-Mone S, Nomane Y, Reymond N, Barbet R, Jacquet E, Imbeaud S, Jacq A, Bouloc P.** 2009. Global analysis of extracytoplasmic stress signaling in Escherichia coli. PLoS Genet. **5**:e1000651. doi:10.1371/journal.pgen.1000651.
15. **Connolly L, De Las Penas A, Alba BM, Gross CA.** 1997. The response to extracytoplasmic stress in Escherichia coli is controlled by partially overlapping pathways. Genes Dev. **11**:2012–2021.
16. **Raivio TL, Silhavy TJ.** 1999. The sigmaE and Cpx regulatory pathways: overlapping but distinct envelope stress responses. Curr. Opin. Microbiol. **2**:159–165.
17. **Vogt SL, Raivio TL.** 2012. Just scratching the surface: an expanding view of the Cpx envelope stress response. FEMS Microbiol. Lett. **326**:2–11.
18. **Dartigalongue C, Missiakas D, Raina S.** 2001. Characterization of the Escherichia coli sigma E regulon. J. Biol. Chem. **276**:20866–20875.
19. **Price NL, Raivio TL.** 2009. Characterization of the Cpx regulon in Escherichia coli strain MC4100. J. Bacteriol. **191**:1798–1815.
20. **Otto K, Silhavy TJ.** 2002. Surface sensing and adhesion of Escherichia coli controlled by the Cpx-signaling pathway. Proc. Natl. Acad. Sci. U. S. A. **99**:2287–2292.
21. **De Wulf P, Kwon O, Lin EC.** 1999. The CpxRA signal transduction system of Escherichia coli: growth-related autoactivation and control of unanticipated target operons. J. Bacteriol. **181**:6772–6778.
22. **Wolfe AJ, Parikh N, Lima BP, Zemaitaitis B.** 2008. Signal integration by the two-component signal transduction response regulator CpxR. J. Bacteriol. **190**:2314–2322.
23. **Engl C, Beek AT, Bekker M, de Mattos JT, Jovanovic G, Buck M.** 2011. Dissipation of proton motive force is not sufficient to induce the phage shock protein response in Escherichia coli. Curr. Microbiol. **62**:1374–1385.
24. **Joly N, Engl C, Jovanovic G, Huvet M, Toni T, Sheng X, Stumpf MP, Buck M.** 2010. Managing membrane stress: the phage shock protein (Psp) response, from molecular mechanisms to physiology. FEMS Microbiol. Rev. **34**:797–827.
25. **Jovanovic G, Lloyd LJ, Stumpf MP, Mayhew AJ, Buck M.** 2006. Induction and function of the phage shock protein extracytoplasmic stress response in Escherichia coli. J. Biol. Chem. **281**:21147–21161.
26. **Jovanovic G, Engl C, Mayhew AJ, Burrows PC, Buck M.** 2010. Properties of the phage-shock-protein (Psp) regulatory complex that govern signal transduction and induction of the Psp response in Escherichia coli. Microbiology **156**:2920–2932.
27. **Rowley G, Spector M, Kormanec J, Roberts M.** 2006. Pushing the envelope: extracytoplasmic stress responses in bacterial pathogens. Nat. Rev. Microbiol. **4**:383–394.
28. **Kobayashi R, Suzuki T, Yoshida M.** 2007. Escherichia coli phage-shock protein A (PspA) binds to membrane phospholipids and repairs proton leakage of the damaged membranes. Mol. Microbiol. **66**:100–109.
29. **Ebel W, Vaughn GJ, Peters HK, 3rd, Trempy JE.** 1997. Inactivation of mdoH leads to increased expression of colanic acid capsular polysaccharide in Escherichia coli. J. Bacteriol. **179**:6858–6861.
30. **Majdalani N, Gottesman S.** 2005. The Rcs phosphorelay: a complex signal transduction system. Annu. Rev. Microbiol. **59**:379–405.
31. **Parker CT, Kloser AW, Schnaitman CA, Stein MA, Gottesman S, Gibson BW.** 1992. Role of the rfaG and rfaP genes in determining the lipopolysaccharide core structure and cell surface properties of Escherichia coli K-12. J. Bacteriol. **174**:2525–2538.
32. **Shiba Y, Yokoyama Y, Aono Y, Kiuchi T, Kusaka J, Matsumoto K, Hara H.** 2004. Activation of the Rcs signal transduction system is responsible for the thermosensitive growth defect of an Escherichia coli mutant lacking phosphatidylglycerol and cardiolipin. J. Bacteriol. **186**:6526–6535.
33. **Laubacher ME, Ades SE.** 2008. The Rcs phosphorelay is a cell envelope stress response activated by peptidoglycan stress and contributes to intrinsic antibiotic resistance. J. Bacteriol. **190**:2065–2074.
34. **Majdalani N, Hernandez D, Gottesman S.** 2002. Regulation and mode of action of the second small RNA activator of RpoS translation, RprA. Mol. Microbiol. **46**:813–826.
35. **Huang YH, Ferrieres L, Clarke DJ.** 2006. The role of the Rcs phosphorelay in Enterobacteriaceae. Res. Microbiol. **157**:206–212.
36. **Castanie-Cornet MP, Cam K, Jacq A.** 2006. RcsF is an outer membrane lipoprotein involved in the RcsCDB phosphorelay signaling pathway in Escherichia coli. J. Bacteriol. **188**:4264–4270.
37. **Hirakawa H, Inazumi Y, Masaki T, Hirata T, Yamaguchi A.** 2005. Indole induces the expression of multidrug exporter genes in Escherichia coli. Mol. Microbiol. **55**:1113–1126.
38. **Nishino K, Honda T, Yamaguchi A.** 2005. Genome-wide analyses of Escherichia coli gene expression responsive to the BaeSR two-component regulatory system. J. Bacteriol. **187**:1763–1772.
39. **Krulwich TA, Sachs G, Padan E.** 2011. Molecular aspects of bacterial pH sensing and homeostasis. Nat. Rev. Microbiol. **9**:330–343.
40. **Edgar R, Bibi E.** 1997. MdfA, an Escherichia coli multidrug resistance protein with an extraordinarily broad spectrum of drug recognition. J. Bacteriol. **179**:2274–2280.
41. **Lewinson O, Adler J, Poelarends GJ, Mazurkiewicz P, Driessen AJ, Bibi E.** 2003. The Escherichia coli multidrug transporter MdfA catalyzes both electrogenic and electroneutral transport reactions. Proc. Natl. Acad. Sci. U. S. A. **100**:1667–1672.
42. **Lewinson O, Padan E, Bibi E.** 2004. Alkalitolerance: a biological function for a multidrug transporter in pH homeostasis. Proc. Natl. Acad. Sci. U. S. A. **101**:14073–14078.
43. **Paulsen IT, Brown MH, Skurray RA.** 1996. Proton-dependent multidrug efflux systems. Microbiol. Rev. **60**:575–608.
44. **Lipinska B, King J, Ang D, Georgopoulos C.** 1988. Sequence analysis and transcriptional regulation of the Escherichia coli grpE gene, encoding a heat shock protein. Nucleic Acids Res. **16**:7545–7562.
45. **Bernhardt TG, de Boer PA.** 2003. The Escherichia coli amidase AmiC is a periplasmic septal ring component exported via the twin-arginine transport pathway. Mol. Microbiol. **48**:1171–1182.
46. **Engl C, Jovanovic G, Lloyd LJ, Murray H, Spitaler M, Ying L, Errington J, Buck M.** 2009. In vivo localizations of membrane stress controllers PspA and PspG in Escherichia coli. Mol. Microbiol. **73**:382–396.
47. **Shimohata N, Chiba S, Saikawa N, Ito K, Akiyama Y.** 2002. The Cpx

stress response system of Escherichia coli senses plasma membrane proteins and controls HtpX, a membrane protease with a cytosolic active site. Genes Cells **7**:653–662.
48. **Cherepanov PP, Wackernagel W.** 1995. Gene disruption in Escherichia coli: TcR and KmR cassettes with the option of Flp-catalyzed excision of the antibiotic-resistance determinant. Gene **158**:9–14.
49. **Datsenko KA, Wanner BL.** 2000. One-step inactivation of chromosomal genes in Escherichia coli K-12 using PCR products. Proc. Natl. Acad. Sci. U. S. A. **97**:6640–6645.
50. **Miller JH.** 1972. Experiments in molecular genetics. Cold Spring Harbor Laboratory, Cold Spring Harbor, NY.
51. **Doerrler WT, Raetz CRH.** 2002. ATPase activity of the MsbA lipid flippase of Escherichia coli. J. Biol. Chem. **277**:36697–36705.
52. **Hiratsu K, Amemura M, Nashimoto H, Shinagawa H, Makino K.** 1995. The rpoE gene of Escherichia coli, which encodes sigma E, is essential for bacterial growth at high temperature. J. Bacteriol. **177**:2918–2922.
53. **Pogliano J, Dong JM, De Wulf P, Furlong D, Boyd D, Losick R, Pogliano K, Lin EC.** 1998. Aberrant cell division and random FtsZ ring positioning in Escherichia coli cpxA* mutants. J. Bacteriol. **180**:3486–3490.
54. **Tsuchido T, VanBogelen RA, Neidhardt FC.** 1986. Heat shock response in Escherichia coli influences cell division. Proc. Natl. Acad. Sci. U. S. A. **83**:6959–6963.
55. **Guisbert E, Yura T, Rhodius VA, Gross CA.** 2008. Convergence of molecular, modeling, and systems approaches for an understanding of the Escherichia coli heat shock response. Microbiol. Mol. Biol. Rev. **72**:545–554.
56. **Duguay AR, Silhavy TJ.** 2004. Quality control in the bacterial periplasm. Biochim. Biophys. Acta **1694**:121–134.
57. **Rouviere PE, De Las Penas A, Mecsas J, Lu CZ, Rudd KE, Gross CA.** 1995. rpoE, the gene encoding the second heat-shock sigma factor, sigma E, in Escherichia coli. EMBO J. **14**:1032–1042.
58. **Danese PN, Silhavy TJ.** 1997. The sigma(E) and the Cpx signal transduction systems control the synthesis of periplasmic protein-folding enzymes in Escherichia coli. Genes Dev. **11**:1183–1193.
59. **Lipinska B, Fayet O, Baird L, Georgopoulos C.** 1989. Identification, characterization, and mapping of the Escherichia coli htrA gene, whose product is essential for bacterial growth only at elevated temperatures. J. Bacteriol. **171**:1574–1584.
60. **Strauch KL, Johnson K, Beckwith J.** 1989. Characterization of degP, a gene required for proteolysis in the cell envelope and essential for growth of Escherichia coli at high temperature. J. Bacteriol. **171**:2689–2696.
61. **Danese PN, Silhavy TJ.** 1998. CpxP, a stress-combative member of the Cpx regulon. J. Bacteriol. **180**:831–839.
62. **Mileykovskaya E, Dowhan W.** 1997. The Cpx two-component signal transduction pathway is activated in Escherichia coli mutant strains lacking phosphatidylethanolamine. J. Bacteriol. **179**:1029–1034.
63. **DeLisa MP, Lee P, Palmer T, Georgiou G.** 2004. Phage shock protein PspA of Escherichia coli relieves saturation of protein export via the Tat pathway. J. Bacteriol. **186**:366–373.
64. **Kleerebezem M, Crielaard W, Tommassen J.** 1996. Involvement of stress protein PspA (phage shock protein A) of Escherichia coli in maintenance of the protonmotive force under stress conditions. EMBO J. **15**:162–171.
65. **Kleerebezem M, Tommassen J.** 1993. Expression of the pspA gene stimulates efficient protein export in Escherichia coli. Mol. Microbiol. **7**:947–956.
66. **Alder NN, Theg SM.** 2003. Energetics of protein transport across biological membranes. A study of the thylakoid DeltapH-dependent/cpTat pathway. Cell **112**:231–242.
67. **Bageshwar UK, Musser SM.** 2007. Two electrical potential-dependent steps are required for transport by the Escherichia coli Tat machinery. J. Cell Biol. **179**:87–99.
68. **Palmer T, Berks BC.** 2012. The twin-arginine translocation (Tat) protein export pathway. Nat. Rev. Microbiol. **10**:483–496.
69. **Doerrler WT, Raetz CRH.** 2005. Loss of outer membrane proteins without inhibition of lipid export in an Escherichia coli YaeT mutant. J. Biol. Chem. **280**:27679–27687.
70. **Sledjeski D, Gottesman S.** 1995. A small RNA acts as an antisilencer of the H-NS-silenced rcsA gene of Escherichia coli. Proc. Natl. Acad. Sci. U. S. A. **92**:2003–2007.
71. **Chen MH, Takeda S, Yamada H, Ishii Y, Yamashino T, Mizuno T.** 2001. Characterization of the RcsC→YojN→RcsB phosphorelay signaling pathway involved in capsular synthesis in Escherichia coli. Biosci. Biotechnol. Biochem. **65**:2364–2367.
72. **Nagahama H, Oshima T, Mori H, Matsumoto K, Hara H.** 2007. Hyperexpression of the osmB gene in an acidic phospholipid-deficient Escherichia coli mutant. J. Gen. Appl. Microbiol. **53**:143–151.
73. **Small P, Blankenhorn D, Welty D, Zinser E, Slonczewski JL.** 1994. Acid and base resistance in Escherichia coli and Shigella flexneri: role of rpoS and growth pH. J. Bacteriol. **176**:1729–1737.
74. **Bulygin VV, Vinogradov AD.** 1991. Interaction of Mg2+ with F0.F1 mitochondrial ATPase as related to its slow active/inactive transition. Biochem. J. **276**(Pt 1):149–156.
75. **Ye JJ, Du J, Lin ZH.** 1989. The effect of Mg2+ on mitochondrial F0.F1 ATPase and characteristics of the nucleotide binding sites. Biochem. Int. **19**:1317–1321.
76. **Mager T, Rimon A, Padan E, Fendler K.** 2011. Transport mechanism and pH regulation of the Na+/H+ antiporter NhaA from Escherichia coli: an electrophysiological study. J. Biol. Chem. **286**:23570–23581.
77. **Padan E, Bibi E, Ito M, Krulwich TA.** 2005. Alkaline pH homeostasis in bacteria: new insights. Biochim. Biophys. Acta **1717**:67–88.
78. **Ledgham F, Quest B, Vallaeys T, Mergeay M, Coves J.** 2005. A probable link between the DedA protein and resistance to selenite. Res. Microbiol. **156**:367–374.
79. **Arai M, Liu L, Fujimoto T, Setiawan A, Kobayashi M.**2011. DedA protein relates to action-mechanism of halicyclamine A, a marine spongean macrocyclic alkaloid, as an anti-dormant mycobacterial substance. Mar. Drugs **9**:984–993.
80. **Zechini B, Versace I.** 2009. Inhibitors of multidrug resistant efflux systems in bacteria. Recent Pat. Antiinfect. Drug Discov. **4**:37–50.
81. **Doerrler WT, Sikdar R, Kumar S, Boughner LA.** 2013. New functions for the ancient DedA membrane protein family. J. Bacteriol. **195**:3–11.